Progress In Electromagnetics Research, PIER 30, 33–46, 2001

EFFICIENT CAPACITANCE COMPUTATION FOR THREE-DIMENSIONAL STRUCTURES BASED ON ADAPTIVE INTEGRAL METHOD

C.-F. Wang, L.-W. Li, P.-S. Kooi, and M.-S. Leong

Department of Electrical and Computer Engineering
The National University of Singapore
10 Kent Ridge Crescent, Singapore 119260

Abstract–The adaptive integral method (AIM) is applied in this paper to calculate the capacitance coefficients for an arbitrarily shaped three-dimensional structure. The uniformity of multipole moment approximation is revealed theoretically and numerically; it is realized that the approach can guarantee the accuracy of AIM for computing capacitance of any structure. The memory requirement and computational complexity of the present method are less than $\mathcal{O}(N^{1.5})$ and $\mathcal{O}(N^{1.5}\log N)$ for three-dimensional problems, respectively. Numerical experiments for several conducting structures demonstrate that the present method is accurate and efficient to compute capacitance of an arbitrarily shaped three-dimensional structure.

1. INTRODUCTION

Capacitance computation for arbitrarily shaped three-dimensional (3D) structures is very important in determining final circuit performance and signal integrity due to the rapid increase in operating frequencies and scales of the circuit systems. In recent years, devel-

opment of various capacitance extractors based on integral equations has become popular. The computation can be carried out by solving a pertinent integral equation using the method of moments (MoM). This procedure is robust and has many advantages over finite difference or finite element schemes, including good conditioning, reduction in dimensionality, and the ability of treating arbitrary regions. However, it has an overriding disadvantage, i.e., the high cost of working with large dense matrix. One of the most powerful methods for the efficient MoM solution is the multilevel fast multipole algorithm (MLFMA) [1, 2], which marries the fast multipole method (FMM) [3–5] and a multilevel-multigrid interpolation concept [6]. MLFMA can reduces the computational complexity and memory requirement to $\mathcal{O}(N \log N)$ for the matrix equation of order N. FastCap and FastHenry [7–9] employ the FMM that was originally developed for particle simulation problems. Another powerful method for the efficient MoM solution is the adaptive integral method (AIM) that has been developed by Bleszynski et al., [10, 11]. Compared to the conventional MoM, AIM reduces computational complexity and memory requirement with the aid of auxiliary basis functions and fast Fourier transform (FFT) that is used in the Precorrected-FFT method [12]. The computational complexities of AIM are $\mathcal{O}(N^{1.5} \log N)$ and $\mathcal{O}(N \log N)$ for surface and volumetric scatterers, respectively. The corresponding memory requirements are $\mathcal{O}(N^{1.5})$ and $\mathcal{O}(N)$, respectively. The AIM has been successfully applied to the analysis of scattering by, and radiation from, arbitrarily-shaped three-dimensional and planar structures [11, 13, 14].

In this paper, we apply the AIM to calculate the capacitance matrix for an arbitrarily shaped 3D structure. The uniformity of multipole moment approximation is examined both theoretically and numerically; it is found that this approach can guarantee the accuracy of AIM for computing capacitance of any structure. Numerical experiments demonstrate that the memory requirement and computational complexity of the present method are less than $\mathcal{O}(N^{1.5})$ and $\mathcal{O}(N^{1.5} \log N)$ for 3D problems, respectively. The present method is thus proven to be efficient to compute capacitance of an arbitrarily shaped 3D structure.

2. FORMULATION

For the standard problem of capacitance computation in three dimensions, we can compute the charge density $\rho(\mathbf{r})$ by solving the following

first-kind integral equation:

$$\phi(\mathbf{r}) = \iint_S G(\mathbf{r}, \mathbf{r}')\rho(\mathbf{r}')d\mathbf{r}' \quad \text{on } S \tag{1}$$

where S denotes the conductor surfaces, $\rho(\mathbf{r})$ is charge density on the conductor surfaces S, $\phi(\mathbf{r})$ is the potential, and $G(\mathbf{r}, \mathbf{r}')$ is the well-known free-space Green's function given by

$$G(\mathbf{r}, \mathbf{r}') = \frac{1}{4\pi\epsilon_0|\mathbf{r} - \mathbf{r}'|}. \tag{2}$$

A standard approach for numerically solving the first-kind integral equation for the charge density $\rho(\mathbf{r})$ is the MoM. In such a approach the conductor surfaces S are approximated by a set of N panels, and it is assumed that on each panel n, a charge, q_n, is uniformly distributed. That is, the charge density $\rho(\mathbf{r})$ is approximated by an expansion in basis functions $f_n(\mathbf{r})$,

$$\rho(\mathbf{r}) = \sum_{n=1}^{N} q_n f_n(\mathbf{r}) \tag{3}$$

where the basis functions $f_n(\mathbf{r})$ are given by

$$f_n(\mathbf{r}) = \begin{cases} 1 & \text{on panel } n, \\ 0 & \text{otherwise.} \end{cases} \tag{4}$$

Applying Galerkin's method results in a matrix equation

$$\mathbf{Z}\,\mathbf{q} = \mathbf{V} \tag{5}$$

in which the matrix $\mathbf{Z} = [Z_{mn}]$ and vector $\mathbf{V} = [V_m]$ can be obtained by the standard Galerkin's procedure.

To develop a fast algorithm for solving the MoM Eq. (5), it is necessary to combine an iterative method with a fast approach to compute the matrix-vector products of the form $\mathbf{Z}\,\mathbf{q}$. In fact, computing $\mathbf{Z}\,\mathbf{q}$ is equivalent to computing the interactions between N sources. The interactions between the sources can be divided into the near and far interactions. The near interactions correspond to a sparse matrix $\mathbf{Z}^{near}$ and $\mathbf{Z}^{near}\mathbf{q}$ is easy to compute. The far interactions correspond to a dense matrix $\mathbf{Z}^{far}$ and the computation of the matrix-vector product

$\mathbf{Z}^{far}\mathbf{q}$ has to be accelerated for an efficient solution. To achieve this acceleration using FFT, the whole structure is enclosed in a rectangular domain that is also known as an auxiliary domain. After discretizing the surfaces S into triangular elements, the auxiliary domain is recursively subdivided into a regular Cartesian grid, so that each small cube contains a few triangular elements at most. In order to perform the matrix-vector product using FFT, we have to translate the original basis functions to the Cartesian grid and this can be done using the basis transformation technique. Based on this idea, the matrix-vector product can be expressed as

$$\begin{aligned}\mathbf{Z}\,\mathbf{q} &= \mathbf{Z}^{near}\mathbf{q} + \mathbf{Z}^{far}\mathbf{q} \\ &= \mathbf{Z}^{near}\mathbf{q} + \mathbf{\Lambda}\,\mathcal{F}^{-1}\left\{\mathcal{F}\{[\,G\,]\}\cdot\mathcal{F}\left\{\mathbf{\Lambda}^T\mathbf{q}\right\}\right\}\end{aligned} \tag{6}$$

in which $[Z_{mn}^{near}] = [Z_{mn}] - [Z_{mn}^{far}]$, $\mathbf{\Lambda}$ is called the basis transformation matrix. The $\mathbf{\Lambda} = [\Lambda_{\alpha\mathbf{u}}]$ can be determined by using the multipole moment approximation criteria [11, 13]. $\mathbf{Z}^{far}$ can be given as following

$$\mathbf{Z}^{far} = \mathbf{\Lambda}\,[G(\mathbf{r}_m, \mathbf{r}_n)]\,\mathbf{\Lambda}^T. \tag{7}$$

From the formulation described above, we can see the significant saving of memory due to the sparsity of matrices $\mathbf{Z}^{near}$ and $\mathbf{\Lambda}$, and the reduction of the CPU time by the utilization of FFT in the matrix-vector product. The memory requirements for $\mathbf{Z}^{near}$, $\mathbf{\Lambda}$, and $[\,G\,]$ are all proportional to $\mathcal{O}(N^{1.5})$. The computational complexity of $\mathbf{Z}^{near}\mathbf{q}$ is proportional to $\mathcal{O}(N)$. The number of unknowns is proportional to the area of object, and the dimension of FFT is proportional to the volume of object; hence, the computational complexity of $\mathbf{Z}^{far}\mathbf{q}$ is $\mathcal{O}(N^{1.5}\log N)$. Thus, the memory requirement and the computational complexity of the formulation described above are $\mathcal{O}(N^{1.5})$ and $\mathcal{O}(N^{1.5}\log N)$, respectively.

3. UNIFROMITY OF MULTIPOLE MOMENT APPROXIMATION

The key point of the present method is how to get the basis transformation matrix $\mathbf{\Lambda}$. Mathematically, the basis functions $f_n(\mathbf{r})$ are approximated as linear combinations of Dirac delta functions,

$$f_n(\mathbf{r}) \simeq \sum_{\mathbf{u}\in C_\alpha} \Lambda_{\alpha\mathbf{u}}\delta^3(\mathbf{r}-\mathbf{u}) \tag{8}$$

localized at expansion box C_α of $(M+1)^3$ nodes, where M is called the order of transformation. The coefficients $\Lambda_{\alpha\mathbf{u}}$ are chosen so as to reproduce the $(M+1)^3$ multipole moments of the basis functions $f_n(\mathbf{r})$,

$$\iiint (x-x_0)^{m_1}(y-y_0)^{m_2}(z-z_0)^{m_3}\left[f_n(\mathbf{r})-\sum_{\mathbf{u}\in C_\alpha}\Lambda_{\alpha\mathbf{u}}\delta^3(\mathbf{r}-\mathbf{u})\right]d\mathbf{r}=0$$
$$\text{for } 0\le m_1,m_2,m_3\le M. \tag{9}$$

The point $\mathbf{r}_0=(x_0,y_0,z_0)$ can be chosen as the center of panel. For this case, it can be shown that the accuracy of multipole moment approximation is independent on the size of object and grid, it depends only on the relative distance between two panels in scale of grid size. This is to say, when we reduce the size of object and grid in same factor, the multipole moment approximation maintains constant accuracy. This uniformity of multipole moment approximation is important to the capacitance computation.

The uniformity of multipole moment approximation mentioned above can be extended to more general cases. The basis functions $f_n(\mathbf{r})$ are assumed to be homogeneous functions: $f_n(\beta\mathbf{r})=\beta^k f_n(\mathbf{r})$. Panels T_m and T_n are reduced to T_m^β and T_n^β in factor of β, respectively. The object and grid are reduced in same factor of β too. We will have the following identity:

$$\begin{aligned}&\iiint_{S^\beta}(x-x_0)^{m_1}(y-y_0)^{m_2}(z-z_0)^{m_3}\left\{f_n(\mathbf{r})-\sum_{\mathbf{u}\in C_\alpha^\beta}\Lambda_{\alpha\mathbf{u}}^\beta\delta^3(\mathbf{r}-\mathbf{u})\right\}d\mathbf{r}\\ &=\beta^{m_1+m_2+m_3+k+3}\iiint_S(x-x_0)^{m_1}(y-y_0)^{m_2}(z-z_0)^{m_3}f_n(\mathbf{r})d\mathbf{r}\\ &\quad-\beta^{m_1+m_2+m_3+3}\sum_{\mathbf{u}\in C_\alpha}\Lambda_{\alpha\mathbf{u}}^\beta(x_u-x_0)^{m_1}(y_u-y_0)^{m_2}(z_u-z_0)^{m_3}.\end{aligned} \tag{10}$$

From above mentioned identity, it is easy to see that the relationship between $\Lambda_{\alpha\mathbf{u}}^\beta$ and $\Lambda_{\alpha\mathbf{u}}$ is as follows:

$$\Lambda_{\alpha\mathbf{u}}^\beta=\beta^k\Lambda_{\alpha\mathbf{u}} \tag{11}$$

With the identity (11), we can derive the following identities:

$$
\begin{aligned}
Z_{mn}^{\beta} &= \iint_{T_m^{\beta}} \iint_{T_n^{\beta}} f_m(\mathbf{r}) G(\mathbf{r},\mathbf{r}') f_n(\mathbf{r}') d\mathbf{r}' d\mathbf{r} \\
&= \beta^{2k+3} \iint_{T_m} \iint_{T_n} f_m(\mathbf{r}) G(\mathbf{r},\mathbf{r}') f_n(\mathbf{r}') d\mathbf{r}' d\mathbf{r} = \beta^{2k+3} Z_{mn} \qquad (12) \\
Z_{mn}^{\beta,far} &= \iint_{T_m^{\beta}} \iint_{T_n^{\beta}} \sum_{\mathbf{u}\in C_m^{\beta}} \Lambda_{m\mathbf{u}}^{\beta} \delta^3(\mathbf{r}-\mathbf{u}) G(\mathbf{r},\mathbf{r}') \sum_{\mathbf{u}\in C_n^{\beta}} \Lambda_{n\mathbf{u}}^{\beta} \delta^3(\mathbf{r}'-\mathbf{u}) d\mathbf{r}' d\mathbf{r} \\
&= \beta^{2k+3} \iint_{T_m} \iint_{T_n} \sum_{\mathbf{u}\in C_m} \Lambda_{m\mathbf{u}} \delta^3(\mathbf{r}-\mathbf{u}) G(\mathbf{r},\mathbf{r}') \sum_{\mathbf{u}\in C_n} \Lambda_{n\mathbf{u}} \delta^3(\mathbf{r}'-\mathbf{u}) d\mathbf{r}' d\mathbf{r} \\
&= \beta^{2k+3} Z_{mn}^{far}. \qquad (13)
\end{aligned}
$$

It is not difficult to get the following identity from (12)–(13):

$$
\left| \frac{Z_{mn}^{\beta} - Z_{mn}^{\beta,far}}{Z_{mn}^{\beta}} \right| = \left| \frac{\beta^{2k+3} Z_{mn} - \beta^{2k+3} Z_{mn}^{far}}{\beta^{2k+3} Z_{mn}} \right| = \left| \frac{Z_{mn} - Z_{mn}^{far}}{Z_{mn}} \right|. \qquad (14)
$$

This is a theoretical proof to the uniformity of multipole moment approximation for homogeneous basis functions that can guarantee the accuracy of AIM for computing capacitance of any structure. We will also prove this uniformity numerically.

4. NUMERICAL RESULTS

In this section, results from computational experiments are presented to demonstrate the efficiency and accuracy of the method described above. The relative error is defined as $Err = ||\mathbf{r}_m||_2 / ||\mathbf{r}_0||_2$. The iteration process will be terminated when the relative error Err falls below 10^{-3}. All experiments were run on HP-C200 workstation.

We can check the accuracy of Z_{mn}^{far} by defining the relative error between Z_{mn} and Z_{mn}^{far} as $\Delta Z_{mn} = |Z_{mn} - Z_{mn}^{far}| / |Z_{mn}|$. Fig. 1 presents the relative error of matrix elements as the function of the distance between the basis and testing functions. Figs. 1(a) and 1(b) show that Z_{mn}^{far} is good enough to approximate the MoM matrix element Z_{mn}. From Fig. 1(b), we can see that Z_{mn}^{far} still keeps almost the same approximate accuracy even though the sizes of the basis and testing functions are reduced by a factor of 100. This example proves the uniformity of multipole moment approximation numerically.

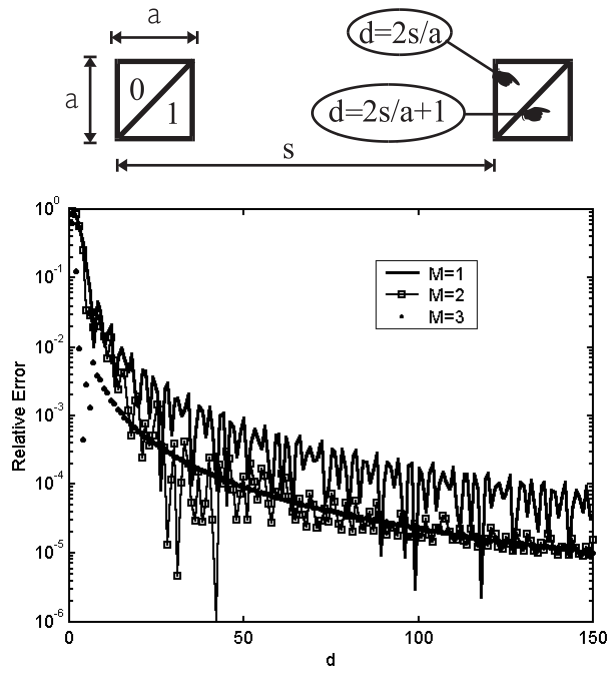

(a) $a = 0.1\,\mathrm{m}$

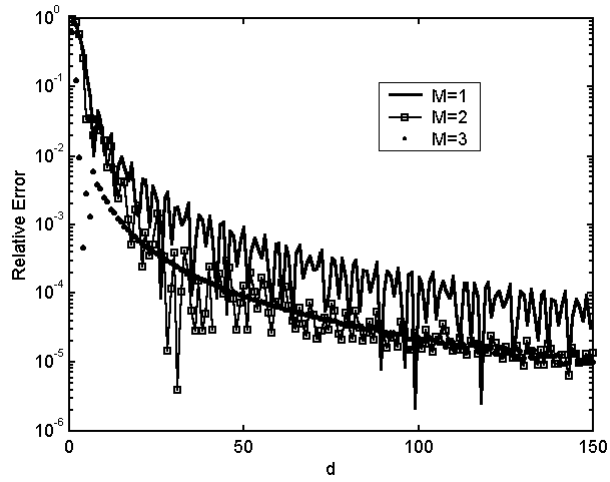

(b) $a = 0.001\,\mathrm{m}$

Figure 1. The relative error in the approximate matrix elements as the function of the distance between the basis and testing functions.

In order to examine the numerical behavior of the method, capacitance of a conducting sphere of radius 1.0 m is considered first. The memory requirement and CPU time per iteration versus the number of unknowns for the conducting sphere of radius 1.0 m are given in Fig. 2. The figure shows that the memory requirement and computational complexity of the present method are less than $\mathcal{O}(N^{1.5})$ and $\mathcal{O}(N^{1.5}\log N)$, respectively. The capacitance of spheres with different radii $R1$ is given in Fig. 3 and is compared with the analytic solution [15]. The results from present method agree with the analytic solution very well.

In the second test case, we consider the capacitance of a two-sphere system. The capacitance of a pair of concentric spherical conducting shells is given in Fig. 3. In this example, the outer radius is fixed to be 1.0 m. The capacitance for different inner radii $R1$ is compared with that of the analytic solution [15]. The capacitance coefficients of two isolated spheres are given in Fig. 4. In this example, we fix radius of one sphere to be 1.0 m and radius of the other one to be 0.75 m. The capacitance coefficients of the system with different distances between two isolated spheres are compared with those of the closed form solutions [16]. All present numerical results agree with the analytic and closed form solutions very well.

In the third test case, we consider the capacitance of a unit cube. The capacitance of the unit cube calculated using the present method is 73.34 pF. The reference results are 73.28 pF and 73.35 pF calculated using preconditioned, adaptive, multipole-accelerated (PAMA) capacitance extraction algorithm [8] and integral equation computer-solution technique [17], respectively. All the three results agree very well. The comparison mentioned above shows that the proposed method has a good accuracy.

In the fourth test case, we consider the capacitance between two thin discs, each of radius 1.0 m and separated by a distance d. For a small d, the capacitance can be given by the Kirchhoff's approximation [18]. The more accurate solution can be found by using integration formulae [19]. The numerical results calculated using the present method are shown in Fig. 5 and compared with those obtained using the Kirchhoff's approximation and integration formula solution. It is seen that our calculated result agrees with that of the integration formula solution very well. Also, Our calculated result agrees with that of the Kirchhoff's approximation very well for small d's. It is

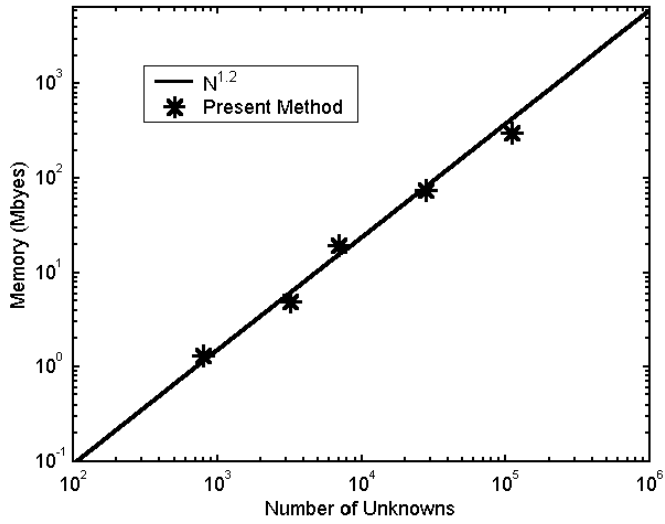

(a)

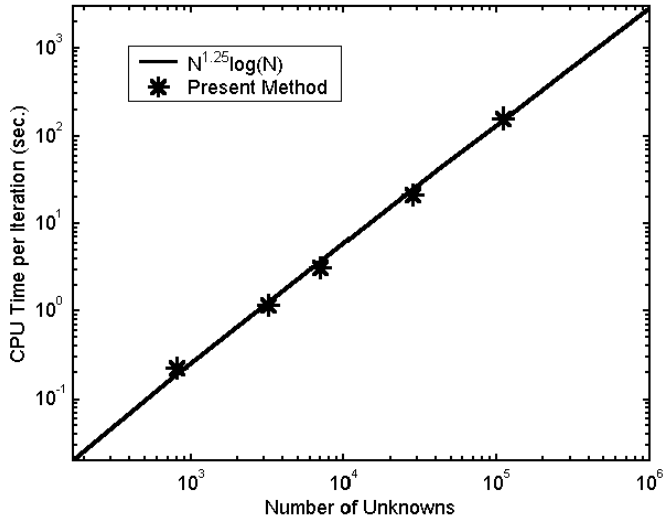

(b)

Figure 2. Computational expense versus the number of unknowns.

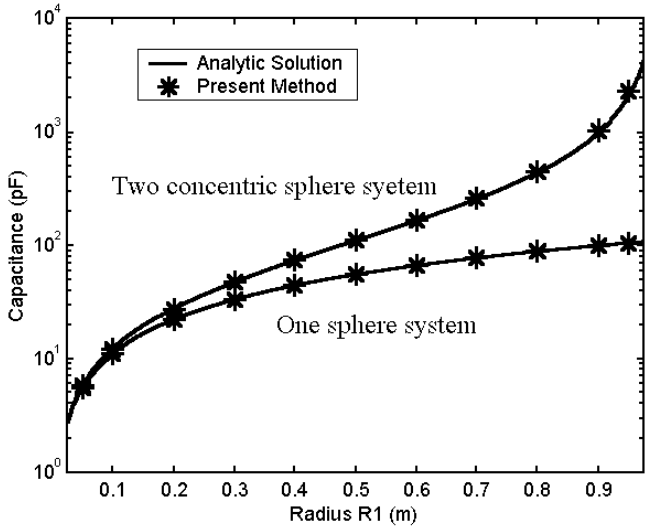

Figure 3. The capacitance of spheres with different radii and the capacitance of a pair of concentric spherical conducting shells with fixed outer radius 1.0 m and different inner radii.

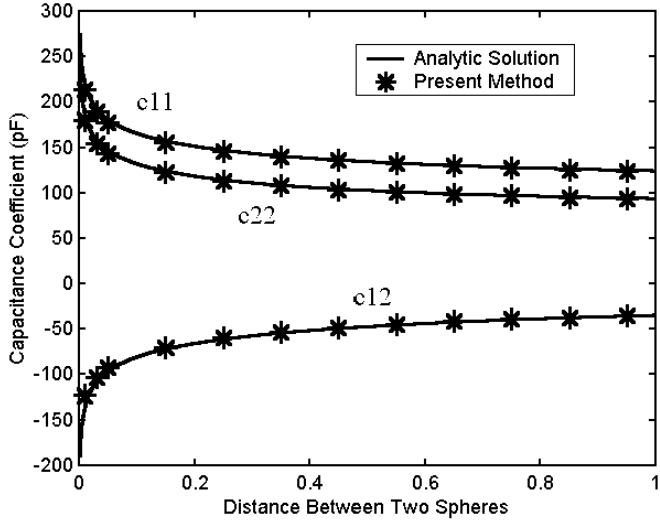

Figure 4. The capacitance coefficients of the system with different distances between two isolated spheres.

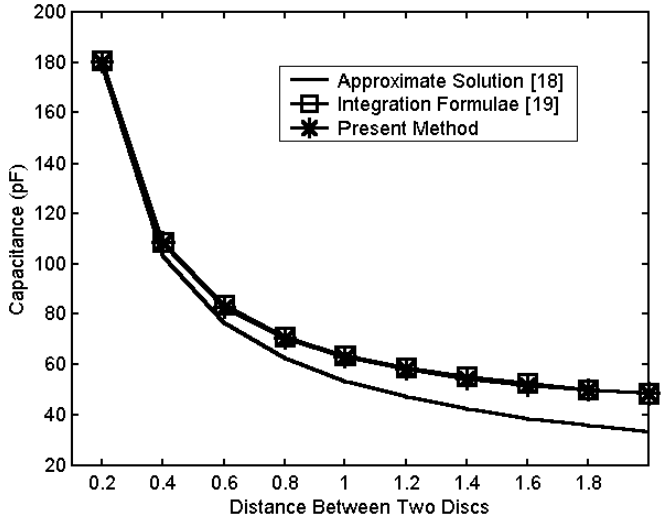

Figure 5. The capacitance of two discs versus the distance between the two discs.

interesting to note that the capacitance approaches the analytic limit 35.5 pF for an infinite separation, whereas the Kirchhoff's approximation 33.55 pF has already passed this limit and hence underestimated the capacitance when $d = 2.0$.

In the last test case, we consider the capacitance coefficients of 2×2 bus structure around a sphere. The geometrical dimensions have been normalized so that bus lines are each 4.0 m long, 1.0 m high, and 1.0 m wide, and all bus line spaces are equally 2.0 m. A conducting sphere of radius 1.0 m is located at the center of bus structure. Fig. 6 shows the charge distribution of the structure when the sphere is charged, while Table 1 presents quantitatively the capacitance coefficients of the structure.

5. CONCLUSION

The AIM has been extended in this paper to calculate the capacitance matrix for an arbitrarily shaped 3D structure. The basis transformation matrix is determined by using certain multipole moment approximation criteria. The uniformity of the multipole moment approximation is revealed theoretically and numerically; and it is found

Table 1. The capacitance coefficients (in pF) of 2×2 bus structure around a sphere.

i	1	2	3	4	5
1	214.01	-5.04	-5.04	-5.04	-5.04
2	-5.04	187.88	-3.14	-2.01	-2.01
3	-5.04	-3.14	187.86	-2.01	-2.01
4	-5.04	-2.01	-2.01	187.87	-3.14
5	-5.04	-2.01	-2.01	-3.14	187.87

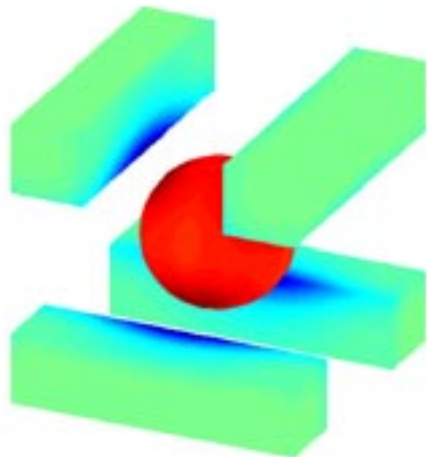

Figure 6. The charge distribution of 2×2 bus structure around a charged sphere.

that this approach can guarantee the accuracy of AIM for computing capacitance of any structure. The memory requirement and computational complexity of the present method are less than $\mathcal{O}(N^{1.5})$ and $\mathcal{O}(N^{1.5} \log N)$ for 3D problems, respectively. Numerical experiments demonstrate that the present method is efficient and accurate for capacitance computation for an arbitrarily shaped 3D structure.

ACKNOWLEDGMENT

This work has been supported in part by research grants from National Science and Technology Board (NUTB), and DSO National Laboratories, of Singapore.

REFERENCES

1. Song, J. M., and W. C. Chew, "Fast multipole method solution using parametric geometry," *Microwave Opt. Tech. Lett.,* Vol. 7, No. 16, 760–765, Nov. 1994.
2. Song, J. M., C. C. Lu, and W. C. Chew, "Multilevel fast multipole algorithm for electromagnetic scattering by large complex objects," *IEEE Trans. Antennas Propagat.,* Vol. 45, No. 10, 1488–1493, Oct. 1997.
3. Greengard, L., *The Rapid Evaluation of Potential Fields in Partial Systems,* MIT Press, Cambridge, MA, 1988.
4. Rokhlin, V., "Rapid solution of integral equation of scattering theory in two dimensions," *J. Comput. Phys.,* Vol. 86, No. 2, 414–439, Feb. 1990.
5. Coifman, R., V. Rokhlin, and S. Wandzura, "The fast multipole method for the wave equation: A pedestrian prescription," *IEEE Antennas Propagat. Mag.,* Vol. 35, No. 3, 7–12, June 1993.
6. Brandt, A., "Multilevel computations of integral transforms and partical interactions with oscillatory kernels," *Comput. Phys. Commun.,* Vol. 65, No. 1–3, 24–38, 1991.
7. Nabors, K., and J. White, "FastCap: A multipole accelerated 3-D capacitance extraction program," *IEEE Trans. Computer-Aided Design,* Vol. 10, No. 11, 1447–1459, Nov. 1991.
8. Nabors, K., S. Kim, and J. White, "Fast capacitance extraction of general three-dimensional structures," *IEEE Trans. Microwave Theory Tech.,* Vol. 40, No. 7, 1496–1506, July 1992.
9. Kamon, M., M. J. Tsuk, and J. White, "FASTHENRY: A multipole-accelerated 3-D inductance extraction program," *IEEE Trans. Microwave Theory Tech.,* Vol. 42, No. 9, 1750–1758, Sept. 1994.
10. Bleszynski, E., M. Bleszynski, and T. Jaroszewicz, "A fast integral equation solver for electromagnetic scattering problems," *IEEE APS Int. Symp. Dig.,* Vol. 1, 416–419, 1994.
11. Bleszynski, E., M. Bleszynski, and T. Jaroszewicz, "AIM: Adaptive integral method for solving large-scale electromagnetic scattering and radiation problems," *Radio Science,* Vol. 31, No. 5, 1225–1251, Sept.–Oct. 1996.

12. Phillips, J. R., and J. White, "A precorrected-FFT method for electrostatic analysis of complicated 3-D structures," *IEEE Trans. Computer-Aided Design of Integrated Circuits and Syst.,* Vol. 16, No. 10, 1059–1072, Oct. 1997.
13. Ling, F., C. F. Wang, and J. M. Jin, "Application of adaptive integral method to scattering and radiation analysis of arbitrarily shaped planar structures," *J. Electromagn. Waves Appl.,* Vol. 12, No. 8, 1021–1037, 1998.
14. Wang, C. F., F. Ling, J. M. Song, and J. M. Jin, "Adaptive integral solution of combined field integral equation," *Microwave Opt. Tech. Lett.,* Vol. 19, No. 5, 321–328, Dec. 1998.
15. Smythe, W. R., *Static and Dynamic Electricity*, Third Edition, A Summa Book, Revised Printing, New York, 1989.
16. Greason, W. D., *Electrostatic Discharge in Electronics*, Research Studies Press Ltd., England, 1992.
17. Ruehli, A. E. and P. A. Brennan, "Efficient capacitance calculations for three-dimensional multiconductor systems," *IEEE Trans. Microwave Theory Tech.,* Vol. 21, No. 2, 76–82, Feb. 1973.
18. Brennan, S. R., *A Dictionary of Applied Physics*, Vol. 2, Electricity, Macmillan, London, 1922.
19. Jaswon, M. A., and G. T. Symm, *Integral Equation Methods in Potential Theory and Elastostatics*, Academic Press, London, 1977.